# Homogeneous surface iron silicide formation on Si(111): The $c(8\times4)$ phase

M. Krause, F. Blobner, L. Hammer, and K. Heinz
*Lehrstuhl für Festkörperphysik, Universität Erlangen-Nürnberg, Staudtstrasse 7, D-91058 Erlangen, Germany*

U. Starke*
*Max-Planck-Institut für Festkörperforschung, Heisenbergstrasse 1, D-70569 Stuttgart, Germany*
*and Lehrstuhl für Festkörperphysik, Universität Erlangen-Nürnberg, Staudtstrasse 7, D-91058 Erlangen, Germany*
(Received 12 February 2003; revised maniscript received 27 May 2003; published 8 September 2003)

The early stages of iron silicide formation on Si(111) were studied by scanning tunneling microscopy (STM), low-energy electron diffraction, and Auger electron spectroscopy. While the initial iron interaction with Si(111) in the submonolayer regime gives rise to inhomogeneous island nucleation, deposition of 1.5 monolayers (ML) iron at room temperature and subsequent annealing at 550–600 °C leads to a flat and homogeneous film with $c(8\times4)$ surface periodicity. This $c(8\times4)$ surface reconstruction is linked to a definite film thickness and thus seems to be stabilized directly through the interface. The film is terminated by a layer of adatoms whose lateral positions form a $(2\times2)$ periodic lattice. At negative tip bias voltages, STM images show an alternating arrangement of darker and brighter adatoms corresponding to the $c(8\times4)$ supercell. While the $(2\times2)$-periodic adatom arrangement develops in a wide temperature regime (450–600 °C) and also for thicker films, the long range ordered $c(8\times4)$ structure can be observed only for 1–2 ML Fe coverage and after high temperature annealing at about 600 °C. Then single $c(8\times4)$ domains can extend to diameters of several hundred nanometers. The atomic structure of the new phase can be derived from a CsCl ($B2$) structure, and a number of structural details are elucidated on the course towards the development of a complete structural model.

DOI: 10.1103/PhysRevB.68.125306 PACS number(s): 68.35.Bs, 68.37.Ef, 68.55.−a

## I. INTRODUCTION

Thin epitaxial iron silicide films on semiconductor material have attracted much attention in view of the potential applications in different technological areas.[1] The interest in these compounds arises, for example, from the hope that $\beta$-$FeSi_2$ might be suitable for optoelectronic devices,[2] since the direct band gap of this orthorhombic phase of 0.85 eV (Refs. 3,4) fits into the window of maximum transmission of optical fibers. Other possible applications are Ohmic contacts,[5] Schottky barriers,[5,6] or nonvolatile memory cells incorporated into the silicon technology.[7] Unfortunately, the most serious problem encountered on the road towards these applications is the growth of films of sufficient homogeneity and crystallinity. Therefore, a better knowledge of the growth mechanism of iron silicide compounds could help to improve the material quality for device applications. Several silicide structures are noted in the bulk phase diagram of iron and silicon,[8] namely, $Fe_3Si$, $\epsilon$-FeSi, $\alpha$-$FeSi_2$, and $\beta$-$FeSi_2$. On the iron rich side $Fe_3Si$ is electrically conducting as well as ferromagnetic and crystallizes in cubic $D0_3$ structure,[9] while $\epsilon$-FeSi is a semimetal with the cubic $B20$ structure.[10] $FeSi_2$ exists in two modifications: the orthorhombic $\beta$-$FeSi_2$,[11] which is semiconducting and stable around room temperature (RT) and the tetragonal $\alpha$-$FeSi_2$.[12] The latter is metallic and stable at high temperatures only, but can be retained by quenching to RT.

For thin films the energetic balance of certain structural phases is modified compared to the bulk since interface, surface and strain energies come into play. Thus, phases not stable in the bulk can be stabilized by epitaxial growth.[13,14] On silicon surfaces for example, distinct metastable thin film structures of different Fe:Si stoichiometries can be prepared.[15–19] Two well ordered silicide film phases have been found so far for iron films below 10 monolayer (ML) thickness on Si(111) resulting upon annealing at different temperatures. They are shown in Figs. 1(a)–1(d) by low-energy electron diffraction (LEED) patterns and scanning tunneling microscopy (STM) images. Between 100 and 300 °C a $(1\times1)$ phase develops with 1:1 composition [Figs. 1(a), 1(b)]. It crystallizes in a silicon terminated cubic CsCl ($B2$) structure[20,21] (so-called $c$-FeSi). A further increase of the annealing temperature to 450–600 °C converts this $(1\times1)$ phase into a $(2\times2)$-periodic structure characterized by $FeSi_2$ stoichiometry [Figs. 1(c), 1(d)]. For this latter phase, three different structural models have been discussed, namely, the abovementioned $\alpha$-$FeSi_2$,[22] the so-called $\gamma$-$FeSi_2$, which has $CaF_2$ ($C1$) structure,[23,24] and a defect modification of the CsCl structure,[25] where half of the iron atoms are removed statistically. $\beta$-$FeSi_2$ evolves only when iron films with coverages exceeding 10 ML are annealed at temperatures of about 600 °C.[19] In LEED it shows a $c(4\times2)$ structure in three rotational domains.[19,26]

There is a clear influence of preparation techniques on the structural and morphological development of the metastable ironsilicide phases.[19] Most commonly a mixture of different phases with heterogeneous morphology develops. This can be understood from the delicate energy balance[16] of the several different phases. Accordingly, not only the energetics of film and interface but also the growth kinetics play an important role for the stabilization of epitaxially grown iron silicide. One key issue for the preparation of uniform and single phase films will certainly be a homogeneous interface. Its preparation as found for other materials may be facilitated

 

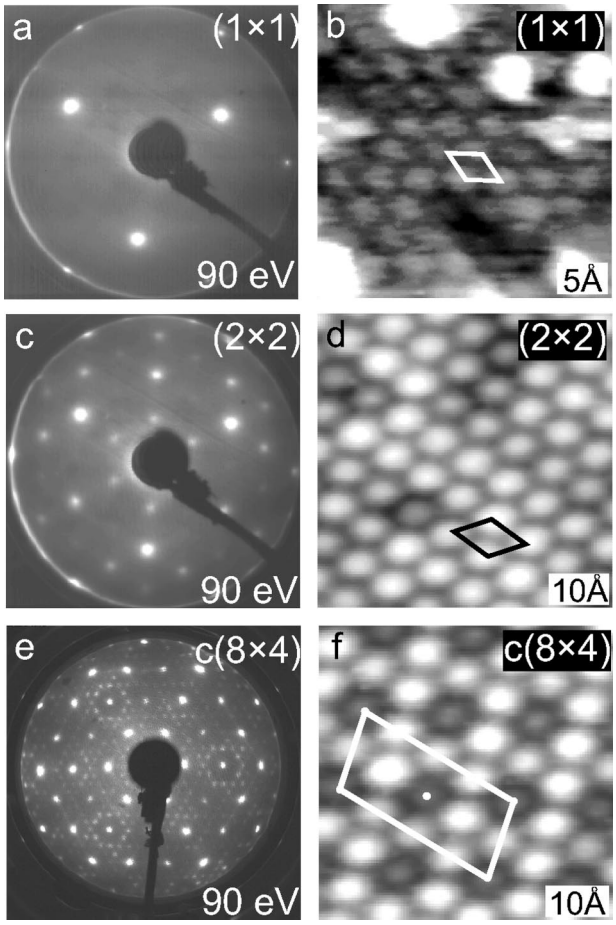


FIG. 1. LEED pattern and STM images of (a), (b) $(1\times1)$; (c),(d) $(2\times2)$; and (e), (f) $c(8\times4)$ phases. All LEED pattern are taken at 90 eV. The STM images are measured with tip bias values of $-1.0$ V (b) and $-1.9$ V (d), (f), the area scanned is indicated by the length scale bars. The corresponding surface unit meshes are added schematically.

by the use of a template.[27,28] The growth of such a thin template layer requires a detailed control of the early stages of deposition and reaction in particular in the case of iron on Si(111), since it is well known that atomic intermixing takes place even when cooling the sample. A number of investigations have been directed towards the early stages of the iron interaction with Si(111),[29–32] however, it appears that no well defined initial layer could be prepared so far. Only at larger film thicknesses, the above mentioned well ordered $(1\times1)$ and $(2\times2)$ phases were obtained.

In the current paper we present a new silicide phase that exists only in the ultrathin film regime. This iron silicide film shows a $c(8\times4)$ surface periodicity as demonstrated in Figs. 1(e), 1(f) by LEED patterns and STM images.[33] It develops as a homogeneous layer with atomically flat terraces extending to several hundred nm, and might be a suitable template for uniform and homogeneous further film growth. Using STM and LEED we determine the preparation conditions and details of the atomic structure of this phase. LEED patterns are used to determine the surface symmetry. From atomically resolved STM images of the $c(8\times4)$ phase—in particular in comparison with the well known Si(111)-$(7\times7)$ reconstruction—we determine adatom registry and step heights between different terraces for structural analysis. After a brief outline of the experiment (Sec. II), the paper describes the morphological development of the flat film (Sec. III) followed by the analysis of thickness, composition, and atomic structure of this two-dimensional silicide phase (Sec. IV). A discussion of the results and a summary conclude the paper.

## II. EXPERIMENT

The experiments were carried out using Si(111) substrates taken from *p*-doped wafers (Bor $10^{15}-10^{16}/\mathrm{cm}^3$). They were oriented within 0.2° with respect to the [111] direction to facilitate the development of large, atomically flat terraces. As judged from terrace widths measured by STM, the orientation in fact must be better than 0.1°. The surfaces were treated *ex situ* in acetone and methanol to remove organic contamination followed by etching with $NH_4F$ to remove the native oxide. Then the samples were introduced through a fast-entry airlock into a home-built ultrahigh vacuum (UHV) apparatus with a base pressure of $2\times10^{-11}$ mbar equipped with an over-head beetle-type STM and a back-view four-grid LEED optics. The same optics was used as retarding field analyzer for Auger electron spectroscopy (AES). The samples could be heated by electron bombardment with the sample holder cooled by liquid nitrogen. After a prolonged outgassing procedure applied to new samples, a clean $(7\times7)$-reconstructed Si(111) substrate was obtained by repeated flashes to 1200 °C in UHV, subsequent quenching to 900 °C, and a further slow cooling at a rate of 0.2 K/s until 800 °C and a rate of 2–4 K/s to RT.[34] Temperatures were measured using an infrared pyrometer. Temperatures below 400 °C were extrapolated based on the heating power. Two electron beam evaporators allowed the simultaneous evaporation of iron and silicon, which could be deposited at variable sample temperatures ($>-170$ °C). However, if not noticed otherwise all presented data will be iron films that have been evaporated at RT or $-170$ °C and annealed afterwards to prepare the silicide phases. Deposition rates were monitored by a quartz microbalance with an error estimated to be about 10%. The pressure during preparation of the $(7\times7)$ reconstruction was in the low $10^{-10}$ mbar range and during Fe deposition about $3\times10^{-11}$ mbar. The films were characterized by STM, LEED, and AES using a sample transfer system so that always the very same phase was subject to the different experimental methods. STM images were acquired at RT at a constant tunneling current of typically 0.5 nA to observe the arrangement of the adatoms of the topmost layer and the morphology of the film. Tungsten tips obtained by electrochemical etching were used. All STM images shown are raw data with no filtering applied except where explicitly noted. For contrast enhancement a slope subtraction algorithm was used. LEED $I(E)$ spectra acquired by a video LEED system[35] were employed as fingerprints to identify identical structures. AES was used to monitor the cleanliness of the sample, as well as the stoichiometry and thickness of the silicide layers.

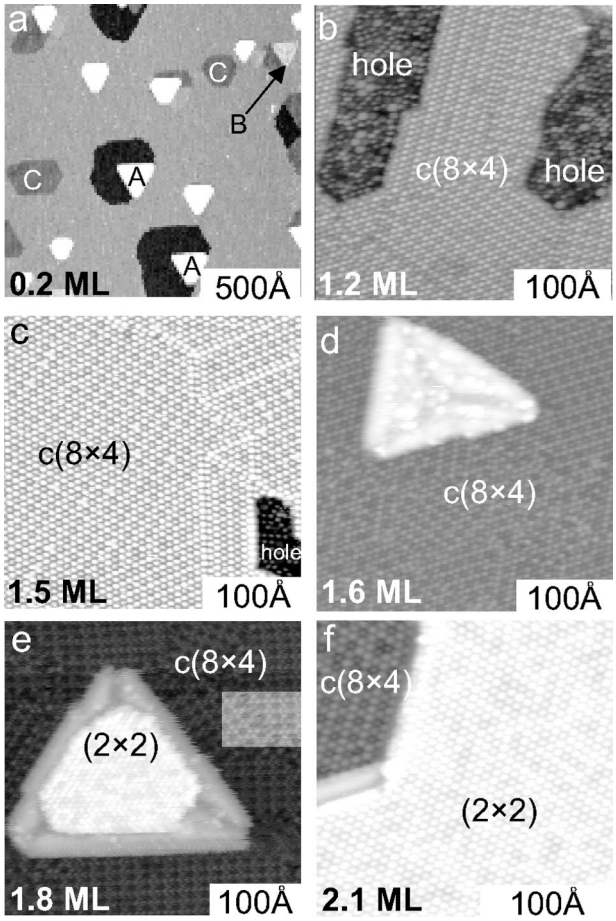


FIG. 2. STM images of the initial iron silicide morphology development showing reacted films between 0.2 and 2.1 ML as indicated in the bottom left of each panel: (a) 0.2 ML with three different types of islands between remains of the Si(111)-(7×7) reconstruction indicated A, B, and C (see text for details, 1500 Å ×1500 Å, $U_{tip}=-1.7$ V); (b) 1.2 ML with $c(8\times4)$ islands and disordered holes (310 Å×310 Å, $U_{tip}=-1.7$ V); (c) 1.5 ML with flat $c(8\times4)$ film (310 Å×310 Å, $U_{tip}=-1.2$ V); (d) 1.6 ML with B-type island on $c(8\times4)$ phase (310 Å×310 Å, $U_{tip}=-2.0$ V); (e) 1.8 ML with B-type island changing to A-type with $(2\times2)$ termination on top of the $c(8\times4)$ film [330 Å×330 Å, $U_{tip}=-0.9$ V, in the inset on the right hand side the contrast is amplified for better visibility of the $c(8\times4)$ structure]; (f) 2.1 ML, $(2\times2)$ displacing more and more $c(8\times4)$ areas (230 Å×230 Å, $U_{tip}=-1.9$ V).

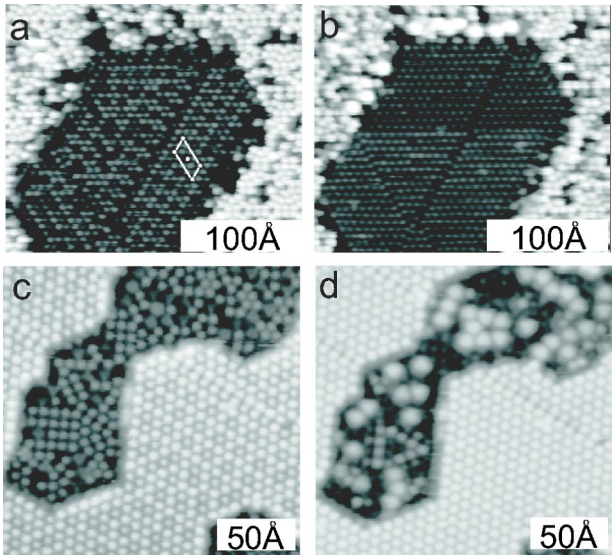


FIG. 3. (a), (b) STM images of a type-C island lying 1.5 Å below the Si(111)-(7×7) reconstruction (coverage: 0.2 ML Fe). (a) At −0.6 V tip bias voltage the $c(8\times4)$ periodicity can be observed, (b) at a tip bias of +0.6 V all adatoms look similar and seem to form a $(2\times2)$-structure. (c), (d) STM images of a hole between $c(8\times4)$-reconstructed areas of the film (coverage: 1.1 ML Fe) taken at (c) −1.4 V and (d) +1.4 V tip bias voltage.

## III. FROM ISLANDS TO A UNIFORM LAYER

### A. Island nucleation

Initial deposition and reaction of iron on Si(111) leads to heterogeneous island nucleation as reported by Köhler and co-workers.[36] At substrate temperatures of about 550 °C which are characteristic for the development of the $(2\times2)$ phase, very mobile iron atoms were observed. In our investigations, which agree with these findings, at coverages as low as 0.05 ML three types of islands were found which were denoted as A, B, and C type.[18,36] Figure 2(a) shows this heterogeneous island nucleation after deposition of 0.2 ML Fe. In this particular experiment the substrate was heated to 550 °C during deposition. Upon that, the (7×7) reconstruction of the substrate remains visible in high resolution STM images in the region between the islands, even though iron diffusion leads to a high local defect density in the adatom layer [see Figs. 3(a), 3(b)]. These (7×7) patches can be used for a comparative evaluation of the island structures: The bright islands in Fig. 2(a), type A, have the shape of equilateral triangles with baselines of typically a few hundred Å length oriented along the $[\bar{1}10]$ directions. These islands tend to grow immediately in multilayers (multiples of 1.6 Å), i.e., three-dimensionally (white areas in the figure). Many of them, especially the expanded ones, are enclosed by depressions with a depth of around 2.8 Å which apparently are etched parts of the silicon layer that serve as Si source for the reaction. A second kind of island, type B, varies from small circular shaped islands with a diameter of about 50 Å to larger triangular shaped islands with rounded edges and lateral dimensions of several 100 Å similar to that of type A. Their height, however, is uniform around 1.6 Å, and—in contrast to type A—they appear not to be connected to depressions. The third type of islands (type C) also shows a strictly two-dimensional growth and normally is sexangular. Type C islands grow 1.5 Å below the adatom height of the (7×7) reconstruction, and can reach diameters between 200 and 500 Å. Island types A and C are terminated by well ordered $(2\times2)$ adatom structures as observed in high resolution STM images. The atomic arrangement on B-type islands can only be well resolved at positive tip bias voltages and appears of limited long range order. However, each island consists of three parts, with boundary stipes running along the $[11\bar{2}]$ substrate directions.

### B. Iron coverage dependent morphology

The presence of the three island types (after annealing to 500–600 °C) proves to be largely independent on the sample temperature during iron evaporation. However, their relative weight changes with increasing iron coverage, as shown in Figs. 2(b)–2(f) for deposition at room temperature and subsequent annealing. The amount of B-type islands decreases, but also three-dimensional growth (A type) seems to be suppressed. As displayed in panel (b), the flat silicide patches (C type) start to spread over the surface and eventually form a closed layer [panel (c)]. While these silicide patches are still terminated by adatoms in $(2\times2)$ periodicity as seen in STM, variation of the tunneling bias reveals the presence of two types of adatom configurations which are characterized by brighter and darker protrusions in empty state images [negative tip bias, see Fig. 1(f)]. These adatoms form a well ordered arrangement corresponding to a $c(8\times4)$ superstructure on the Si(111) substrate which is also observed by LEED [see Fig. 1(e)]. Detailed inspection of the C-type islands in the initial heterogeneous growth regime also discloses this bias dependent $c(8\times4)$ periodicity as shown in Figs. 3(a) and 3(b), and corroborates the interpretation that it is indeed this island type that eventually covers the whole surface. Below 1.5 ML the $c(8\times4)$ patches are interrupted by shallow holes [see Fig. 2(b) at 1.2 ML]. Figures 3(c) and 3(d) depict one of these holes to contain two different kinds of atoms which are poorly ordered. Atoms of the one kind have next neighbors at similar distances as the adatoms in the ordered $c(8\times4)$ areas and appear to lie 1.2 Å to 1.4 Å below those (depending on tip bias voltage). Atoms of the other kind have a next neighbor distance of about 10 Å and appear to cover a larger area each. The appearance of this second kind of atoms shows a strong bias dependence which causes a contrast reversal between both atomic types upon reversing the tunneling direction. The apparent height of the second type ranges from 1.8 Å (at $-1.4$ V tip bias voltage) to 0.4 Å (at $+1.4$ V) below the $c(8\times4)$ adatoms [see Figs. 3(c) and 3(d)]. This bias dependence is most likely due to chemical contrast, which suggests that the holes contain both Si and Fe atoms, but the amount of iron seems to be insufficient to form a $c(8\times4)$ structure. Eventually, at about 1.5 ML, the holes have almost completely disappeared as shown in Fig. 2(c). The $c(8\times4)$ patches form a continuous layer with three rotational domains on a typical length scale of 100 to 300 Å. At higher initial iron coverage, the $c(8\times4)$ patches are accompanied by a new kind of silicide island with atomic disorder on the surface similar to B-type ones [see Figs. 2(d) and 2(e)], until at 2 ML and above large $(2\times2)$ areas are formed without this distinct bias dependence of their adatom appearance which correlates those to A-type islands [see Fig. 2(f)].

### C. Thermal stability of the $c(8\times4)$ phase

The $c(8\times4)$ ordering and the development of $(2\times2)$-periodic adatoms on the surface obviously proceed at different temperatures indicative of different activation energies for these two aspects of this large scale reconstruction. Figure 4 displays STM images recorded after annealing at

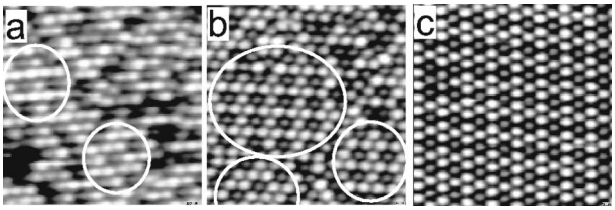


FIG. 4. STM images (115 Å×115 Å each) of films containing 1.5 ML of Fe annealed at different temperatures, (a) 500 °C, (b) 550 °C, (c) 600 °C. Circles in (a) and (b) indicate the $c(8\times4)$ ordered areas. Long range ordering of the $c(8\times4)$ structure is obtained only at 600 °C.

500, 550, and 600 °C. The adatoms are already visible at 500 °C (a), even dark and bright atoms can be observed at this temperature. An onset of a short-range correlation between dark and bright atoms occurs around 550 °C (b) with local $c(8\times4)$ units already visible in the STM image. However, the long-range ordering in large $c(8\times4)$ domains requires a temperature of about 600 °C (c) and only then a LEED pattern develops exhibiting the 1/4- and 1/8-order spots. An interesting observation is that the $c(8\times4)$ structure appears to be thermally more stable than the $(2\times2)$ phase observed for thicker films. From Fe/Si peak-to-peak ratios of the AES intensities monitored for increasing temperature (not displayed) for an initial iron coverage of 1.5 ML [at which the $c(8\times4)$ phase develops] and 4 ML Fe+8 ML Si coevaporated [for which the $(2\times2)$ film is found], we determine that the plateau characteristic for the stable high temperature film extends to only 550 °C in the $(2\times2)$ case and up to 650 °C for the $c(8\times4)$ structure.

## IV. FILM COMPOSITION AND ATOMIC STRUCTURE

As shown in the previous paragraph, the amount of $c(8\times4)$-reconstructed areas in the submonolayer regime increases with the initial iron coverage until a closed $c(8\times4)$ layer is reached at about 1.5 ML. Exceeding this critical coverage, type A and type B islands grow on the expense of the flat layer. This suggests, that the $c(8\times4)$ reconstructed film or the type C island, respectively, have a definite thickness. However, even at 1.5 ML Fe the silicide film is not completely flat on a large scale. In contrast, original terraces of the clean Si(111) surface, which are delimited by more or less straight step edges in a distance of 300–1000 nm (on this particular area of the sample), are split up into a two levels percolation structure. The structures formed have characteristic lengths of the order of 100 nm, and their edges are strongly meandering [see Figs. 5(a), 5(b)].

### A. Film height and composition

The detailed inspection of an atomically resolved image of the boundary between two adjacent $c(8\times4)$ terraces of different height provides further insight into the atomic properties of the $c(8\times4)$ phase. The terrace boundaries between two such levels often contain small $(7\times7)$-Si(111) remnants as shown in Fig. 5(c) and later in Fig. 7. The difference between the two $c(8\times4)$ terrace heights is determined from

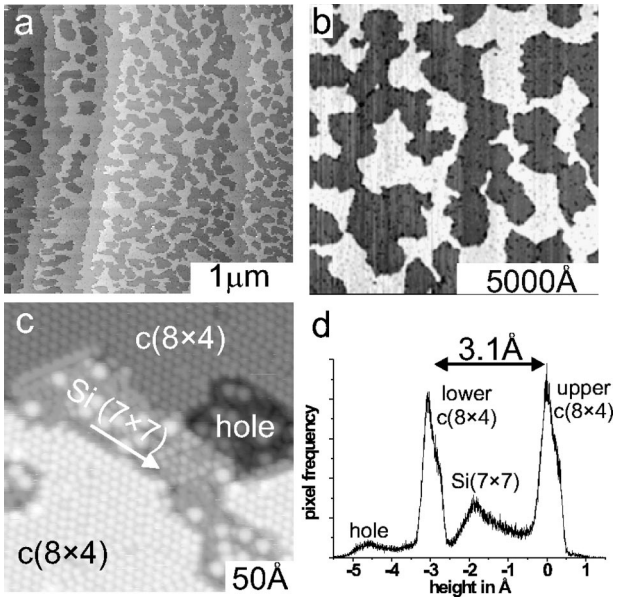


FIG. 5. (a) STM image of a $c(8\times4)$ film on adjacent substrate terraces, (b) meandering iron silicide films with two different levels of $c(8\times4)$ reconstruction (coverage 1.5 ML Fe). White: upper level (58%), gray: lower level (42%) ($U_{tip}=-1.9$ V). (c) Details of step between upper and lower terrace. (d) Corresponding image histogram ($U_{tip}=1.4$ V).

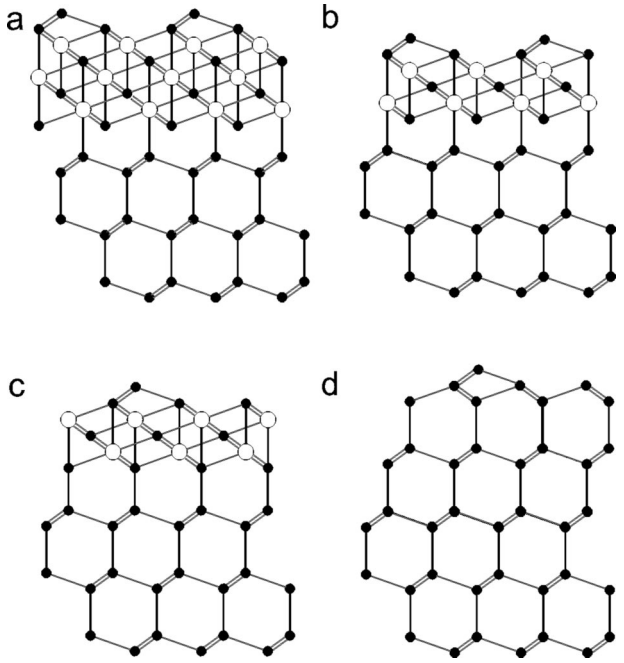


FIG. 6. Side view models of two layer and three layer silicide interfaces, (a) 3B8, (b) 2B8, and (c) 2B7. (d) displays a part of the $(7\times7)$-Si(111) unit cell. Bonds within the $\{\bar{1}10\}$ projection plane are drawn as single lines, double lines indicate two bonds directed by 60° into and out of the plane. Large open spheres correspond to Fe atoms, small dark spheres to Si atoms.

STM image histograms [see Fig. 5(d)] to be 3.1 Å. Similarly, we can measure the step height between the $c(8\times4)$ terraces and the $(7\times7)$ adatom level. Of course, the values vary slightly with the tunneling voltage, since here electronic effects play a certain role. From the lower $c(8\times4)$ patch to the $(7\times7)$ patch we find a step height in the range of 1.2 to 1.7 Å, which is the same as found for C-type islands embedded in the Si substrate at submonolayer coverages. Correspondingly, from the $(7\times7)$ band to the next $c(8\times4)$ level the vertical distance is 1.4–1.9 Å.

As noted, the high temperature film phase [in $(2\times2)$ periodicity for thicker films] represents $FeSi_2$ resulting from 50% iron depletion of 1:1 stoichiometric FeSi in CsCl structure.[19] Transferring this model to the $c(8\times4)$ structure which ideally contains 1.5 ML iron would correspond to three layers of such an $FeSi_2$ as depicted by the sketch in Fig. 6(a).[37] (An additional Si layer is included at the interface.) In this model a Si-Fe-Si surface termination was chosen in analogy to the $(1\times1)$-FeSi film and covered by additional Si adatoms (0.25 ML). This $(1\times1)$ phase has a true CsCl structure and is terminated by a Si layer.[20,21] Yet, already in the regime of optimum preparation of the $(1\times1)$ phase, the appearance of isolated adatoms was observed on top of this Si layer [see Fig. 1(b)] which eventually leads to the $(2\times2)$ periodic adatom arrangement, and thus suggests a similar terminating layer sequence for the two phases. Additional support for the layer sequence of our model is drawn from a quantitative evaluation of the AES data with the intensities calculated according to the composition for each layer and their respective escape depths considered angular dependent since an RFA was used for data collection. The inelastic mean free path values were taken as 4 Å for 47 eV and 5 Å for 92 eV.[38] A normalization to the known structure of the $(1\times1)$ phase accounts for matrix factors and the spectrometer function. The experimental[39] intensity ratio Fe/Si of the $c(8\times4)$ phase fits within 15% to our model (a satisfactory agreement in view of the assumptions) while other feasible termination scenarios such as an Fe termination or an additional Si monolayer or bilayer deviate by more than 50%. Nevertheless, for the model chosen neither the restriction to 1.5 ML nor the nature of the adatom corrugation difference within the $c(8\times4)$ unit cell are immediately apparent. Yet, since it is not a priori evident, that the $c(8\times4)$ structure represents $FeSi_2$ stoichiometry as the $(2\times2)$ phase does for thicker films at comparable temperatures, a deviating stoichiometry with a two or four layer silicide is also conceivable. Comparison of the experimental step heights with the corresponding distances for different possible film models corroborates the idea of a two silicide layer model as we will see below. The interplay of coverage and thickness for this model makes the presence of different adatom coordinations appear more feasible, which will also be discussed in detail in the following section.

For a theoretical estimate of the height change upon silicide formation we need to evaluate the thickness difference between the silicide layer and the Si substrate slab which has been replaced. For the Si substrate, we have to consider the thickness of the Si layers used for silicide formation plus the additional value contributed by the $(7\times7)$ reconstruction. The available ingredients concerning the silicide film are the interface spacing, the thickness of the silicide itself and the additional contribution by the adatom layer. The vertical

spacing at the interface depends on the type of interface iron coordination. For a cubic silicide based on the CsCl structural type on a Si(111) substrate, three coordination configurations are commonly considered and solely feasible. Depending on the silicide bonding to the topmost substrate bilayer one may find eightfold or sevenfold iron coordination as shown in Figs. 6(b), 6(c). In the case where the lowest Si layer of the silicide is missing, the eightfold type [see Fig. 6(b)] converts into a fivefold coordination (not shown). However, the Si-Fe interface bond length would not be affected, so that the fivefold type can be represented by the eightfold type in the present consideration of just vertical spacings. Also, the in-plane orientation of the silicide with respect to the substrate, which can be realized in two ways for each coordination type (so-called A and B interface type), can be neglected. It should be noted, however, that from theoretical[21] and experimental[40] work a B8 coordination is preferred for CsCl and $CaF_2$ film structures. Accordingly B-type interfaces are displayed in Fig. 6. Thus, by assuming an unrelaxed Si-Fe bond length of 2.34 Å at the very interface (which is the theoretical bulk value for $CaF_2$ type silicide[41]) one obtains two possible spacings between the two Si layers, namely, of 1.56 Å at the A8- or B8-type interface, whereas at the A7- or B7-type interface they should have the spacing of a Si-Si bond of about 2.35 Å (bulk value of Si). Of course, the bond lengths and layer spacings at the interface can be relaxed considerably. However, one knows e.g., from the $CoSi_2$/Si(111) interface[42,43] that oscillatory contractions and expansions to a large extent cancel each other, so that the average layer spacing approximately corresponds to the respective bulk values. For the case of iron silicide this has been shown to hold also for *c*-FeSi (0.04 Å deviation).[21] Since the lattice mismatch between the different silicide models is very small, the thickness of the silicide film itself can also be evaluated using the theoretical values for the $CaF_2$-type silicide.[41] This yields a layer spacing of 0.78 Å in a potential CsCl defect-type silicide. An iron/silicon layer stack (our previous definition of a CsCl type layer) accordingly corresponds to a vertical height of 1.56 Å.

Information on the surface termination of the silicide can be inferred from the gradual development of the $(2\times2)$ adlayer on top of $(1\times1)$-FeSi. The latter has been determined to be of CsCl-type crystal structure with a Si-layer surface termination.[20,21] As already visible in the STM image of this $(1\times1)$ phase [Fig. 1(b)], singular adatoms appear on top of this layer which eventually form a $(2\times2)$ pattern with increasing temperature. Therefore, it seems very likely that the adlayers of the $(2\times2)$ or $c(8\times4)$ phases reside on top of a terminating Si layer, corresponding to a general trend for silicide surfaces.[16] For the thickness of the $(2\times2)$ adatom layer on the silicide we have no safe value as its exact nature is not known. However, the low reactivity and sensitivity to residual gas point towards Si atoms, which apparently are threefold coordinated as shown in the next paragraph. Thus, one would expect values not much different from those in the $(7\times7)$ reconstruction on Si(111) which are 1.19–1.30 Å for the different adatoms in the $(7\times7)$ unit cell.[44] For the $(\sqrt{3}\times\sqrt{3})R30°$-B/Si(111) phase with Si adatoms above boron (which in turn is incorporated into the first Si bilayer)

TABLE I. Estimated values for layer spacings in silicide layer, interface, and Si substrate.

| | $(7\times7)$-Si(111) | eight-type silicide | seven-type silicide |
|---|---|---|---|
| Si bilayer (BL) | 3.13 Å[a] | | |
| "eff." recon. BL | 3.05 Å[b] | | |
| adatom layer | 1.19–1.30 Å[b] | 1.15–1.34 Å[c] | 1.15–1.34 Å[c] |
| silicide layer | | 1.56 Å[d] | 1.56 Å[d] |
| interface (Si-Si) | | 1.56 Å[d] | 2.35 Å[a] |

[a]Si bulk values.
[b]From LEED analysis (Ref. 44).
[c]Values for $(\sqrt{3}\times\sqrt{3})R30°$-B/Si(111) (Refs. 45,46).
[d]Theoretical bulk values for $FeSi_2$ ($CaF_2$ structure) (Ref. 41).

values of 1.15 and 1.34 Å as adatom heights have been reported.[45,46] With a more accurate account lacking it seems appropriate to assume the same adatom layer thickness for the two compared phases and—on account of the scatter of the values for these other systems—to note an estimated error of about $\pm0.2$ Å. The reconstructed layers of the $(7\times7)$-Si(111) surface consist of the just discussed adatom layer and one additional reconstructed bilayer defining the faulted and unfaulted halves of the unit cell [see Fig. 6(d) for a sketch of part of a faulted half]. The latter obviously is thicker than a Si bilayer in the bulk of 3.13 Å. The LEED analysis reported values of 3.39–3.49 Å for the different positions in the $(7\times7)$ unit cell.[44] However, the subsequent bilayer is compressed to 0.37–0.40 Å, which approximately compensates the expansion. So an effective value for *a single* (topmost) reconstructed bilayer results as 3.05 Å. The layer spacings as discussed above for the evaluation of the step height between $c(8\times4)$ and $(7\times7)$ terraces are summarized in Table I.

A judgement of the electronically caused differences between the apparent height of the adatom layers on the silicide and on the $(7\times7)$-Si(111) surface is difficult. A conservative estimate can be drawn from the variation in STM of the experimental step heights with tunneling bias. Combined with the unknown true height of the silicide adatoms (see above) we estimate an uncertainty of about $\pm0.35$ Å. It

TABLE II. Theoretical heights for steps (positive=rising) from $(7\times7)$ to $c(8\times4)$ terraces for different silicide models ($n$B7, $n$B8) and thicknesses ($n=2$–4) assuming rigid layer spacings as function of number of silicon bilayers (BL) used up. Good agreement to the experimental values is indicated by the boldfacing of vertical pairs.

| Si consumption | step heights estimated for different interface models and film thicknesses (all numbers given in Å) | | | | | |
|---|---|---|---|---|---|---|
| | 2B8 | 2B7 | 3B8 | 3B7 | 4B8 | 4B7 |
| 1BL | **+1.63** | +2.42 | +3.19 | +3.98 | +4.75 | +5.54 |
| 2BL | **−1.50** | −0.71 | +0.06 | +0.85 | **+1.62** | +2.41 |
| 3BL | −4.63 | −3.84 | −3.07 | −2.28 | **−1.51** | −0.72 |

should be kept in mind that this estimate is not based on a quantitative error evaluation but rather on plausibility considerations.

Step heights estimated from these elementary values are listed in Table II for two-, three- and four-layer silicide models in seven- and eight-type coordination for different amounts of Si consumption (1, 2, and 3 bilayers). Clearly, the only combinations compatible with the experimental values of $-1.2$ to $-1.7$ Å and $+1.4$ to $+1.9$ Å are eightfold coordinated interfaces and film thicknesses of two or four silicide layers. For three silicide layers as well as sevenfold type interface coordination the deviations are significantly beyond the error estimate. This result immediately indicates that the $c(8\times4)$ silicide is of a different stoichiometry than proposed for the $(2\times2)$ phase in thicker films, since at 1.5 ML iron such a 1:2 composition, or 50% occupation of iron sites in the CsCl lattice, would require three silicide layers. To the contrary, in two and four silicide layers 1.5 ML iron atoms would occupy 75 or 37.5 % of the iron sites, respectively. For several reasons the two-layer model appears more likely than the four-layer one. Firstly, type C islands, or equally the lower $c(8\times4)$ patches, are formed below the $(7\times7)$ level. For a four-layer silicide that would imply that the reaction immediately reaches down to the third substrate bilayer—and is stopped there abruptly. One would expect to observe thickness deviations and find three- or five-layer thick patches, which is not the case. Secondly, for an iron depletion down to 37.5% one might expect the CsCl structure to become instable, since there is no stable silicide phase reported below $FeSi_2$ stoichiometry (corresponding to an iron depletion of 50% on average) and the solubility of iron in the fcc Si lattice is extremely low. Thirdly, since the new $c(8\times4)$ phase develops only at an iron content of 1.5 ML its stability seems to be mediated by the interface itself. Such an effect is unlikely when the respective film is more than 6 Å thick, as also indicated by recent theoretical studies for the $(1\times1)$ phase.[21] Finally, we want to mention that derived from adatom positions an additional argument in favor of the two layer silicide model will be given in the next subsection.

Last but not least, the large scale morphology of the films corroborates the two layer model: the generation of a two-layer silicide with its 3 ML of Si should consume 1.5 bilayers of the Si substrate, since the adatom density is practically the same in the $c(8\times4)$ phase and the $(7\times7)$ reconstruction (only a slight deficit arises from the cornerholes). Consequently, we have to expect a half-and-half mixture of one and two bilayer consumption, which is exactly represented by the up and down terraces in equal ratio displayed in Fig. 5(b). The average size of the percolation structure indicates that large mass transport over distances of about 1000 Å is involved in the silicide reaction process.

### B. Registry, adatom position, and ordering

In the last paragraph we have assigned the $c(8\times4)$ film to be a two-layer silicide derived from the CsCl structure with an average occupancy of only 3/4 for Fe sites. On the course towards a complete structural model for the film we need to determine the local position of the $(2\times2)$ arranged adatoms. Also we have to find a suitable film structure giving rise to their different appearance in STM, which eventually leads to the development of the $c(8\times4)$ superperiodicity. In a first attempt one can try to derive the adatom position on the $c(8\times4)$ silicide film from direct STM imaging of defects, i.e., where adatoms are locally missing. Indeed, at such isolated positions STM can resolve the layer below the adlayer, which has $(1\times1)$-symmetry with the adatoms seemingly positioned in threefold coordinated hollow sites. However, since these holes are small, influences of the tip shape might invalidate such an assignment. On the other hand, single adatoms are also observed already on top of the $(1\times1)$ CsCl film, which evolves with annealing temperatures below 300 °C [see Fig. 1(b)]. In that case the adatoms clearly occupy threefold hollow sites of the underlying atomically resolved $(1\times1)$ lattice. Due to the gradual formation of the $c(8\times4)$ phase at higher annealing temperatures, its local adatom configuration is expected to be the same. Nevertheless it would be preferable to have a direct proof for the threefold hollow site derived from the undisturbed $c(8\times4)$ structure. Additionally, one needs to discriminate between two alternatives. In threefold coordination, the adatoms could reside either above the Fe atoms of the first Fe layer or above the Si atoms in the second Si layer ($T4$ or $H3$ sites, respectively,[47] Fig. 6 shows $T4$ site adatoms). This information can be derived from a triangulation method using as a reference the known adatom structure and registry to the substrate of the clean Si(111)-$(7\times7)$ patches, which are found at step edges as noted earlier. The adatoms of the $(7\times7)$ reconstruction are known to reside in $T4$ coordination and the lateral registry of the adatoms is well defined by the underlying substrate. From bias dependent STM images of the $(7\times7)$ patch the faulted and unfaulted halves of the unit cell can be identified as shown in Figs. 7(a), 7(b). The faulted half appears brighter in images showing the filled states.[48] Thus we know the orientation of the substrate layers and in turn the lateral registry shift between different layers. By projecting a $(1\times1)$ grid on the adatom positions of the $(7\times7)$ area we find the adatoms of the upper $c(8\times4)$ terrace to be shifted by $(-1/3,-1/3)$ in $[\bar{1}\bar{1}2]$ direction or a third of the unit cell diagonal $D/3$ as displayed in Figs. 7(c)–7(e). From a side view model in the respective orientation, i.e. parallel to the $(\bar{1}10)$ plane as shown in Fig. 7(g) we can now determine the adatom position in the silicide. However, as a crucial point of this analysis, we need to assume a certain interface stacking. As already outlined, experimental as well as theoretical results[21,40] clearly point towards a B-type stacking, which therefore is taken over in the following. In Fig. 7(g) a part of the faulted half of the $(7\times7)$ unit cell is displayed in the middle section of the model. There, the adatoms reside directly above the atoms of the lowest atomic plane displayed. The respective grid positions in the upper $c(8\times4)$ island are represented by the topmost Si layer of the silicide. Thus it can be concluded that the registry shift of the adatoms in $[\bar{1}\bar{1}2]$ direction by $-D/3$ corresponds to a $T4$ site, which is also visualized in a top view [see Fig. 7(e)].

The same triangulation procedure can be done between both the elevated and the depressed $c(8\times4)$ regions as shown in Fig. 7(f). In that case the overlayed grid depicts a registry shift of $(+1/3,+1/3)$ between the two. This assigns the adatoms of the lower $c(8\times4)$ patch to the same positions as in the $(7\times7)$ band which further corroborates the model drawn in Fig. 7(g) [the lower $c(8\times4)$ patch is displayed at the left edge of the side view]. It should be noted that the $T4$ adatom site determination would remain valid even if the topmost full Si layer would be again stacked with a 180° rotation (B type). Finally we mention that the same registry analysis, when applied to a 4B8 silicide model [see Fig. 7(g), right side], would result in $T1$ adatom positions, i.e., they would reside on top of the topmost Si layer atoms of the film, which is very unlikely and consequently again rules out the four-layer silicide model.

Since the adatoms reside above the Fe positions, their local electronic density of states and probably their vertical positions as well should be noticeably influenced by vacancies underneath, i.e., missing atoms (defects) in the Fe layer. So it is tempting to assign the different appearance of adatoms within the $c(8\times4)$ unit cell to an ordering of vacancies within the topmost iron layer. Of course, adatoms situated on top of an iron atom would exhibit a different geometrical height and even more a deviating electronic structure as compared to those situated above a defect site. However such a model raises some problems since the number of defects within the unit cell is much higher than the number of corresponding adatoms. The primitive unit cell designated by the matrix $\left(\begin{smallmatrix}4 & 2\\ 0 & 4\end{smallmatrix}\right)$ contains 32 Fe positions in the whole film and correspondingly 8 vacancies, while it includes only one dark and three bright adatoms. Since the energetics of an adatom site above an Fe atom should be very different from that above a defect site, a strong driving force would be required for the respective arrangement of vacancies below particular (dark or bright) adatoms. Such an enforcement can only be envisioned by a rather complex defect structure within the silicide film. Though this cannot be *a priori* dismissed there is at least no equivalence in silicide bulk structures.

Further insight in the local configuration of adatoms can be gained from preliminary density functional theory (DFT) calculations performed in our group.[49] In these calculations Si adatoms in a $(2\times2)$ periodic arrangement were put on top of a Si-terminated surface of FeSi with CsCl structure and fully relaxed. Note, that such adatoms are indeed observed experimentally in the lower temperature regime, though they are not ordered as assumed in the calculation. As a result, the most favorable adsorption site for the adatoms turns out to be the $H3$ hollow site with about 0.5 eV lower in energy than the $T4$ site right above the Fe atoms. (Note, that the top site configuration of adatoms results in more than 2 eV higher binding energy, again ruling out the four-layer silicide model.) Moreover, even the most favorable adatom site turns out to be higher in energy than the uncovered surface irrespective of the choice of the chemical potential, which needs to be introduced as a further parameter in order to account for the different stoichiometries of the systems compared. Following this evaluation no adatoms at all should be found on a FeSi film, which is in clear contrast to experimental observations. The only solution is that even in the $(1\times1)$ phase some singular vacancies within the topmost Fe layer exist which are decorated by adatoms. Their local configuration on a defect $T4$ site to a large extent resembles that of a $H3$ site and might be even more favorable. Transferring the results to the $c(8\times4)$ structure it hardly seems probable that any of the adatoms would reside on top of an Fe atom, since

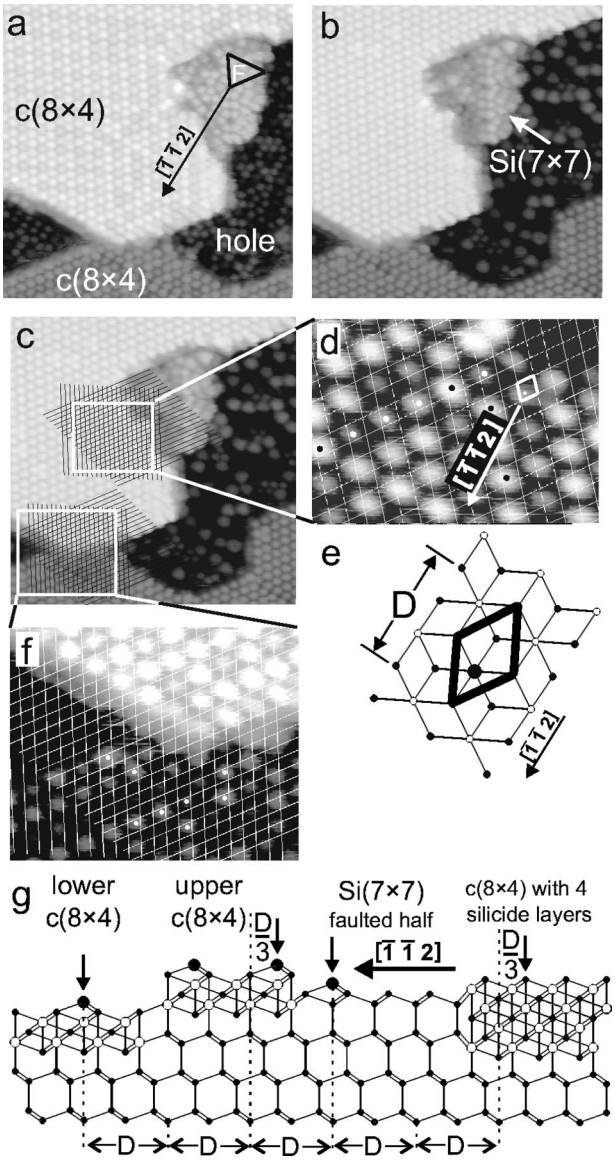


FIG. 7. STM image of upper and lower $c(8\times4)$ levels with an area of residual $(7\times7)$ reconstruction [250 Å×250 Å, (a) $U_{tip}=-0.6$ V, (b) $U_{tip}=+0.6$ V]. (c) Two overlayed grids depict the registry shift between adatoms of the (d) $(7\times7)$ and upper $c(8\times4)$ structures and (e) upper $c(8\times4)$ and lower $c(8\times4)$ structures. (f) Top view of the three topmost silicide layers and registry shift of adatom according to STM images. (g) Side view model of two $c(8\times4)$ levels with $(7\times7)$ band in between. Bonds within the $\{\bar{1}10\}$ projection plane are drawn as single lines, double lines indicate two bonds directed by 60° into and out of the plane. Large open spheres correspond to Fe atoms, small dark spheres to Si atoms.

the energy cost of more than half an eV appears to be by far too high to become overcompensated by the energy gain from mere ordering of defects within the silicide film. Thus, we have to assume that all of the adatoms within the $c(8\times4)$ structure indeed reside above defect sites, which consumes about half of the vacancies available in the whole film. The other half, however, must then be responsible for the observed STM contrast of adatoms via indirect, lattice-mediated interactions. The same argument holds of course in all cases, where adatoms of different STM appearance are observed, i.e. for the disordered stage preceding the $c(8\times4)$ ordering [see Fig. 4(a)] as well as for thicker $(2\times2)FeSi_2$ films [see Fig. 2(f)]. The problem now is to arrange the four remaining vacancies within the primitive unit cell of the $c(8\times4)$ structure (or 3–5 vacancies, taking the experimental uncertainty in the determination of the Fe content into account) in a certain way among the two Fe layers so that the observed periodicity is reproduced. If they would all be in the upper Fe layer in between the already present $(2\times2)$ ordered defects below the adatoms, this would hardly lead to the required decoration of one of the adatoms, since all Fe sites available are situated right in the middle of two neighboring adatoms. Only an extreme disproportion in their distribution would account for that which has no obvious physical reason, since in such a model both the underlying $(1\times1)$ periodic interface and the $(2\times2)$ surface structure would not enforce such a highly symmetry-breaking arrangement. Therefore, it is by far more reasonable to place at least part of the defects also right at the interface. Unfortunately, the local configuration of a defect at the interface is hardly predictable. So, it is not clear whether then lower coordinated Si atoms around the B8-coordinated defect site remain stable at all. As a consequence, severe local restructuring may arise involving even substitution or place exchange of Fe and Si atoms. This, in combination with local lattice strain induced correspondingly, might lead to a complex reconstruction network at the interface. However, neither the structure nor the energetics of such an interface reconstruction can be sufficiently modeled at the present stage and further experimental as well as theoretical work is required for a detailed understanding.

## V. DISCUSSION

In the previous paragraphs, it was shown that a stable $c(8\times4)$ reconstruction exists in the regime of ultrathin iron silicide films. The most striking observation is the specific iron content required for a homogeneous development of this phase. A well ordered $c(8\times4)$ phase is formed only upon deposition of just 1.5 ML Fe. The films described in the previous paragraphs were prepared from an iron film initially deposited at RT or $-170\,^{\circ}C$ followed by annealing at approximately $600\,^{\circ}C$. It should be noted, however, that the $c(8\times4)$ phase can also be prepared by simultaneous (co)deposition of 1.5 ML Fe and 3 ML Si. The silicide reaction resulting in the $c(8\times4)$ structure is obviously limited to a certain depth. But it also immediately proceeds to this definite depth, i.e., the thickness of the $c(8\times4)$ phase, and only at 1.5 ML iron the full surface reacts. At lower Fe exposure the $c(8\times4)$ silicide film is interrupted by holes with a disordered atomic arrangement due to an incomplete silicide reaction and quite rarely also small patches of the clean silicon $(7\times7)$ phase occur. Above 1.5 ML, a different type of silicide, namely, the $(2\times2)$ phase grows in islands ontop of the $c(8\times4)$ film. The silicide reaction then requires additional silicon that has to diffuse through the already reacted film. This diffusion presumably is concentrated to domain or grain boundaries in the film or to substrate steps, thus leading to the observed island formation [see Figs. 2(d), 2(e)].

Based on well resolved step height measurements in STM images, composition and film thickness of the $c(8\times4)$ phase could be determined unambiguously. Even though the layer spacings used for this evaluation were bulk values, theoretical distances or values taken from similar systems, our result is clearly significant based on the error estimate. It is a configuration of two incompletely filled Fe layers and three Si layers. A comparison of the film composition, e.g., to bulk silicides, is difficult, since the interface and adlayer Si influences its evaluation. Nonetheless, we obtain the *differential* stoichiometry of the film, if we only consider an inner film double layer (defect CsCl structure). That would correspond to $Fe_{1.5}Si_2$ or $Fe_3Si_4$ which is not a stable composition in the bulk phase diagram. The reason why the $c(8\times4)$ phase prefers this particular configuration is not yet clear, but it must be due to a direct interaction of surface and interface structure, which appears quite likely for such a thin film.

The adatom position assignment is based on a few assumptions, which, however, are convincingly reasonable. First, of course, we rely on the correctness of the two-layer silicide model. Secondly, the assumption of a B8 interface configuration is based on theoretical investigations for the $(1\times1)$ low-temperature FeSi phase and on experimental findings for thick $(2\times2)$ $FeSi_2$ films, it has not been determined independently for the $c(8\times4)$ phase itself. The film structure being a CsCl-type cubic structure is also not *a priori* clear, but intuitively suggestive since all other ultrathin film phases have been proven to be cubic. Last but not least, the correct orientation of the substrate can safely be fixed by the identification of faulted halves in the $(7\times7)$ unit cell. The resulting $T4$ site is in good agreement with a variety of adatom systems on Si(111), as well as on silicide films. However, DFT calculations do not favor such a site in the present case leading to the model of associated Fe vacancies below the adatoms.

Long before the two types of adatoms develop the well ordered mutual arrangement leading to the $c(8\times4)$ phase, the $(2\times2)$ periodic corrugation caused by the adatoms is present at the surface. Even at that early stage bright and dark adatoms can be identified in STM, which, however, are randomly disordered within the $(2\times2)$ lattice. In fact, a $(2\times2)$-type short range correlation is already visible in the disordered adlayer on the low temperature $(1\times1)$ phase (not shown) indicating the presence of Fe vacancies even at that stage. Obviously the $(2\times2)$ adatom configuration is thermodynamically stable and kinetically easily accessible, since the Si atoms required are readily available from substrate steps via surface diffusion. The development of the $c(8\times4)$ phase, to the contrary, requires an ordered arrange-

ment of the remaining defects below the surface and most probably at the very interface. As we can deduce from STM measurements, that proceeds in two steps: first, the defects need to be created, which takes place already below 450 °C. That seems to proceed easily and is possibly caused by the particular thinness of the film. The second step, ordering of the defects, requires Fe interdiffusion within the film or even a complete long-range interface reconstruction, which is obviously hindered by a large activation barrier. However, once established, the structure is very stable as seen by the higher disintegration temperature. STM images show that only above 650 °C the film morphology changes and again islands are formed with a $(2\times2)$ adatom termination. In that process the $c(8\times4)$ periodicity is lost. Possibly this conversion requires the availability of additional Si from the substrate which due to the homogeneity of the $c(8\times4)$ phase can only diffuse via domain or grain boundaries. This causes the higher conversion temperature on the one hand, and on the other hand leads to a rough morphology and island formation.

Finally we speculate that the homogeneous film phase in the $FeSi_2$ stoichiometry regime on Si(111) as discovered with the $c(8\times4)$ film structure could serve as a template for further homogeneous growth and eventually lead to good $\beta$-$FeSi_2$ films. The latter displaying a $c(4\times2)$ periodicity on the Si(111) surface would directly fit on the $c(8\times4)$ phase. If it is possible to isolate single orientation domains of the $c(8\times4)$ phase, e.g., by way of pinning to substrate terraces of appropriate width, the anisotropy of both film phases might help to generate single domain $\beta$-$FeSi_2$ material for optoelectronic applications. Still at isolated steps of the flat sample used in the present investigation such an orientation preference could not be observed.

## VI. SUMMARY

The high temperature phase (450–600 °C) of ultrathin iron silicide films on Si(111) turns out to be more complicated than previously believed. The structural and morphological development displays a delicate coverage dependence. While in the submonolayer regime immediately islands of three different structural types develop, at 1.5 ML initial iron coverage only one of the structures takes over. It forms a flat film containing a well ordered $c(8\times4)$ reconstruction in large domains. The surface loses its homogeneity again at higher iron coverages and develops $(2\times2)$ domains of different height. A noticeably higher temperature stability of the $c(8\times4)$ phase is observed. Taking into account the pronounced coverage dependence for a perfect development of the $c(8\times4)$ silicide a structural model can be deduced from STM height measurements. In addition to the adatoms visible in STM the film contains three Si and two incompletely filled Fe layers forming a structure based on the CsCl type. Atomically resolved images of the $c(8\times4)$ phase and adjacent $(7\times7)$ reconstructed patches of the Si(111) surface allow to assign the adatom position to $T4$ sites, i.e., directly above the iron positions of the second film layer. Energetic arguments point towards Fe vacancies below every adatom, while their dark and bright appearance in STM images is assigned to an ordering of the remaining vacancies most likely at the interface.

## ACKNOWLEDGMENTS

Support by the Deutsche Forschungsgemeinschaft (DFG) is gratefully acknowledged.

*Email address: u.starke@fkf.mpg.de

[1] J. Derrien, J. Chevrier, V. Le Thanh, T.E. Crumbaker, J.Y. Natoli, and L. Berbezier, Appl. Surf. Sci. **70/71**, 546 (1993).
[2] H. Lange, Phys. Status Solidi B **201**, 3 (1997).
[3] M. De Crescenzi, G. Gaggiotti, N. Motta, F. Patella, A. Balzarotti, and J. Derrien, Phys. Rev. B **42**, 5871 (1990).
[4] N.E. Christensen, Phys. Rev. B **42**, 7148 (1990).
[5] S.P. Murarka, *Silicides for VLSI Applications* (Academic Press, Orlando, 1983).
[6] E. Rosencher, S. Delage, and F.A. d'Avitaya, J. Vac. Sci. Technol. B **3**, 762 (1985).
[7] R. Kläsges, C. Carbone, W. Eberhardt, C. Pampuch, O. Rader, T. Kachel, and W. Gudat, Phys. Rev. B **56**, 10 801 (1997).
[8] M. Hansen, *Constitution of Binary Alloys* (McGraw-Hill, New York, 1958).
[9] Y.P. Selisskij, Structure Rep. **10**, 17 (1945).
[10] L. Pauling and A.M. Soldate, Acta Crystallogr. **1**, 212 (1948).
[11] Y. Dusausoy, J. Protas, R. Wandji, and B. Roques, Acta Crystallogr., Sect. B: Struct. Crystallogr. Cryst. Chem. **27**, 1209 (1971).
[12] F.A. Sidorenko, P.V. Geld, and L.B. Dubrovskaya, Phys. Met. Metallogr. **8**, 134 (1959).
[13] D.M. Wood and A. Zunger, Phys. Rev. B **40**, 4062 (1989).
[14] H. von Känel, E. Müller, S. Goncalves-Conto, C. Schwarz, and N. Onda, Appl. Surf. Sci. **104/105**, 204 (1996).
[15] A.L. Vazquez de Parga, J. de la Figuera, C. Ocal, and R. Miranda, Europhys. Lett. **18**, 595 (1992).
[16] E.G. Michel, Appl. Surf. Sci. **117/118**, 294 (1997).
[17] U. Kafader, P. Wetzel, C. Pirri, and G. Gewinner, Appl. Phys. Lett. **63**, 2360 (1993).
[18] W. Weiß, M. Kutschera, U. Starke, M. Mozzafari, K. Resthöft, U. Köhler, and K. Heinz, Surf. Sci. **377-379**, 861 (1997).
[19] U. Starke, W. Weiss, M. Kutschera, R. Bandorf, and K. Heinz, J. Appl. Phys. **91**, 6154 (2002).
[20] S. Walter, R. Bandorf, W. Weiss, K. Heinz, U. Starke, M. Straß, M. Bockstedte, and O. Pankratov, Phys. Rev. B **67**, 085413 (2003).
[21] S. Walter, M. Krause, F. Blobner, S. Müller, U. Starke, and K. Heinz, J. Phys: Condens. Matter **15**, 5207 (2003).
[22] N. Jedrecy, A. Waldhauer, M. Sauvage-Simkin, R. Pinchaux, and Y. Zheng, Phys. Rev. B **49**, 4725 (1994).
[23] N. Onda, J. Henz, E. Müller, H. von Känel, C. Schwarz, and R.E. Pixley, Helv. Phys. Acta **64**, 197 (1991).
[24] H. von Känel, R. Stadler, H. Sirringhaus, N. Onda, and J. Henz, Appl. Surf. Sci. **53**, 196 (1991).
[25] H. von Känel, K.A. Mäder, E. Müller, N. Onda, and H. Sirringhaus, Phys. Rev. B **45**, 13 807 (1992).
[26] A.L. Vazquez de Parga, J. de la Figuera, J.E. Prieto, C. Ocal, and R. Miranda, Appl. Phys. A: Mater. Sci. Process. **57**, 477 (1993).

[27] S.M. Yalisove, R.T. Tung, and D. Loretto, J. Vac. Sci. Technol. A **7**, 1472 (1989).
[28] R. Stadler, C. Schwarz, H. Sirringhaus, and H. von Känel, Surf. Sci. **271**, 355 (1992).
[29] H. Moritz, B. Rösen, S. Popovic, A. Rizzi, and H. Lüth, J. Vac. Sci. Technol. B **10**, 1704 (1992).
[30] J. Alvarez, A.L. Vazquez de Parga, J.J. Hinarejos, J. de la Figuera, E.G. Michel, C. Ocal, and R. Miranda, Phys. Rev. B **47**, 16 048 (1993).
[31] W. Raunau, H. Niehus, T. Schilling, and G. Comsa, Surf. Sci. **286**, 203 (1993).
[32] A. Mascaraque, J. Avila, C. Teodorescu, M.C. Asensio, and E.G. Michel, Phys. Rev. B **55**, R7315 (1997).
[33] The designation $c(8\times4)$ represents a nonprimitive surface unit cell. The corresponding primitive cell is described by the matrix $\left(\begin{smallmatrix}4 & 2\\ 0 & 4\end{smallmatrix}\right)$.
[34] B.S. Swartzentruber, Y.-W. Mo, M.B. Webb, and M.B Lagally, J. Vac. Sci. Technol. A **7**, 2901 (1989).
[35] K. Heinz, Rep. Prog. Phys. **58**, 637 (1995).
[36] M. Mozzafari, K. Resthöft, and U. Köhler, Verh. Dtsch. Phys. Ges. **31**, 1805 (1996).
[37] We define one silicide layer in CsCl structure as the stack of one Si and one Fe layer—the latter also containing iron vacancies.
[38] S. Tanuma, C.J. Powell, and D.R. Penn, J. Vac. Sci. Technol. A **8**, 2213 (1990).
[39] U. Starke, S. Walter, M. Krause, F. Blobner, R. Bandorf, W. Weiß, S. Müller, L. Hammer, and K. Heinz, in *Atomic Structure of Ultrathin Iron Silicide Films on Si(111): Metastable Phases and a New Template Structure*, edited by M. J. Aziz *et al.*, MRS Symposia Proceedings No. 749 (Materials Research Society, Warrendale, PA, 2002), W5.3.
[40] E. Müller, D.P. Grindatto, H.-U. Nissen, N. Onda, and H. von Känel, Appl. Phys. Lett. **64**, 1938 (1994).
[41] E.G. Moroni, R. Podloucky, and J. Hafner, Phys. Rev. Lett. **81**, 1969 (1998).
[42] A. Seubert, J. Schardt, W. Weiß, U. Starke, K. Heinz, and Th. Fauster, Appl. Phys. Lett. **76**, 727 (2000).
[43] R. Stadler, D. Vogtenhuber, and R. Podloucky, Phys. Rev. B **60**, 17 112 (1999).
[44] S.Y. Tong, H. Huang, C.M. Wei, W.E. Packard, F.K. Men, G. Glander, and M.B. Webb, J. Vac. Sci. Technol. A **6**, 615 (1988).
[45] P. Baumgärtel, J.J. Paggel, M. Hasselblatt, K. Horn, V. Fernandez, O. Schaff, J.H. Weaver, A.M. Bradshaw, D.P. Woodruff, E. Rotenberg, and J. Denlinger, Phys. Rev. B **59**, 13 014 (1999).
[46] H. Huang, S.Y. Tong, J. Quinn, and F. Jona, Phys. Rev. B **41**, 3276 (1990).
[47] Threefold hollow adatom positions are commonly denoted $T4$ for on top of a second layer atom, thus effectively fourfold coordinated, and $H3$ for true hollow site and threefold coordinated.
[48] R.J. Hamers, R.M. Tromp, and J.E. Demuth, Surf. Sci. **181**, 346 (1987).
[49] S. Walter, Ph.D. thesis, University Erlangen-Nürnberg, 2003.